Zeeman effect in the phosphorescence spectra of complex molecules in disordered media under selective excitation

B. M. Kharlamov, E. I. Al'shitz, and R. I. Personov

Institute of Spectroscopy, Academy of Sciences of the USSR, Moscow
(Submitted 27 March 1984)
Zh. Eksp. Teor. Fiz. **87**, 750–762 (September 1984)

A new method has been developed for studying the Zeeman effect in the phosphorescence spectrum of complex molecules in isotropic solid solutions with inhomogeneously broadened spectra. The method is based on the removal of inhomogeneous broadening by selective laser $T_1 \leftarrow S_0$ excitation, and on the examination of the intensity distribution in the quintets produced in the spectrum (when an external magnetic field is applied). The intensity distribution in the Zeeman quintets is analyzed theoretically in the presence and absence of Boltzmann equilibrium, and it is shown that experimental data can be used to find the zero-field radiative deactivation constants of spin sublevels as well as the spin-lattice relaxation constants. The experiments were performed with coronene and 5-Br-acenaphthene in fields up to 50 kOe ($T \approx 5$ K). The relative rates of radiative zero-field deactivation of spin sublevels have been measured, and the rates of spin-lattice relaxation in different fields have been found for 5-Br-acenaphthene.

INTRODUCTION

In addition to singlet electronic levels S_n, the molecules of organic compounds also have a set of excited triplet levels T_n. The lowest triplet level T_1 is metastable and plays an important role in photophysical, photochemical, and biological processes. The $T_1 \rightarrow S_0$ optical transitions are responsible for the phosphorescence of organic molecules.

Studies of the Zeeman effect in phosphorescence spectra[1] are an important source of information about the spin structure and properties of triplet states. However, in the case of complex organic molecules in solution, such studies are fundamentally restricted by the considerable width of their spectral bands (100–1000 cm^{-1}), which usually exceeds the Zeeman splitting by two or three orders of magnitude.

It has now been established that, in many cases, and at sufficiently low temperatures, the formation of broad bands in the spectra of solutions of organic compounds is dominated by inhomogeneous broadening due to differences between the local conditions for the different molecules in the solid host.[2,3] The last decade has seen the development of methods for removing this broadening and for exhibiting the "true" fine structure of fluorescence, phosphorescence, and absorption spectra by selective laser excitation of centers of a particular type (see the review by Personov[4] and the references therein). Inhomogeneous broadening in phosphorescence spectra can be removed by selective $T_1 \leftarrow S_0$ excitation.[5] The line spectra observed under these conditions contain particularly narrow pure electronic lines (their width is 0.1–0.2 cm^{-1} at 4.2 K). This has ensured that the zero-field splitting of lines due to the spin-spin magnetic dipole interaction has been recorded directly in the optical spectrum of a complex molecule for the first time.[6] It is clear that this situation provides favorable conditions for detailed studies of the Zeeman effect in complex molecules in arbitrary magnetic fields from $H = 0$ upward. Some preliminary results of such experiments are briefly reported in Ref. 7 and 8.

In this paper, we present the results of detailed studies of the Zeeman effect in complex molecules in isotropic solid solutions under selective laser $T_1 \leftarrow S_0$ excitation. We have carried out a theoretical analysis of the structure of the spectrum with allowance for the specificity of the object, namely, spatial disorder and strong inhomogeneous broadening. We have carried out an experimental study of compounds with different triplet-state lifetimes. Finally, we have demonstrated new ways of using experimental data to determine the parameters of triplet states and spin-lattice relaxation rates.

THEORETICAL ANALYSIS

We begin by analyzing the general appearance of the phosphorescence spectrum of molecules in a magnetic field under strong inhomogeneous broadening which is removed by selective $T_1 \leftarrow S_0$ excitation. It will be sufficient to confine our attention to the region of purely electronic transitions because the picture is repeated in the longer wavelength part of the phosphorescence spectrum.

1. General principles. Consider a system of identical noninteracting molecules (in an isotropic solid solution) in a constant external magnetic field. We shall suppose that the field is strong enough to ensure that the Zeeman splitting is considerably greater than the zero-field splitting of the triplet level T_1. The Zeeman splitting will be assumed to be the same for all the molecules in solution. However, owing to differences between local conditions, the positions of the triplets due to the individual molecules will be subject to a statistical spread along the energy scale. It follows that, under monochromatic $T_1 \leftarrow S_0$ excitation, the laser will "select" three types of center in the inhomogeneous system, each of which will be excited to one of its Zeeman sublevels (Fig. 1a). Nonradiative transitions between Zeeman sublevels in each center will then result in the population of the other two sublevels as well. The emission spectrum of each type of cen-
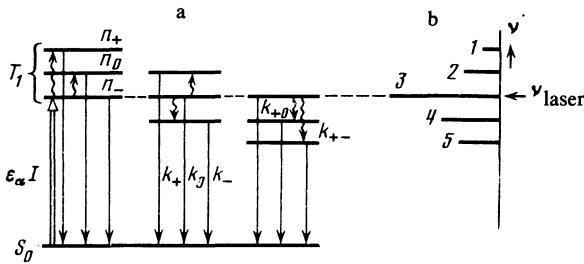
FIG. 1. Level scheme illustrating the origin of the Zeeman quintet in the phosphorescence spectrum of an isotropic solution under selective $T_1 \leftarrow S_0$ excitation: a—Zeeman sublevels of three types of center excited by the laser radiation; b—quintet appearing in the spectrum.

ter will contain three lines. The overall phosphorescence spectrum (due to the emission of all three types of laser excited center) will contain a quintet because some of the components of triplets of different centers will coincide (Fig. 1b).

It is clear that the intensity distribution in the Zeeman quintet must depend strongly on the spin-lattice relaxation

rates. When this relaxation is completely absent, the spectrum should contain only the central line of the quintet (line 3 in Fig. 1b). Let us consider the intensity distribution in the Zeeman multiplet in greater detail.

The Hamiltonian for two electrons with resultant spin S in an external magnetic field H can be written in the form[1,9]

$$\hat{H} = g\beta \mathbf{HS} - (XS_x{}^2 + YS_y{}^2 + ZS_z{}^2), \tag{1}$$

where β is the Bohr magneton, $g = 2$, and X, Y, Z are the energies of spin sublevels in zero external fields.[1] We can use this Hamiltonian to show that, when the external magnetic field is strong (so that the Zeeman splitting is much greater than the zero-field splitting; this occurs for $H \gtrsim 10$ kOe), the corrections to the energies of the spin sublevels are

$$W_1 = 0, \qquad W_{2,3} = \pm g\beta H, \tag{2}$$

and the corresponding spin wave functions T_+, T_0, T_- in the magnetic field H can be expressed in terms of the zero-field functions T_x, T_y, T_z as follows:

$$\begin{pmatrix} T_+ \\ T_0 \\ T_- \end{pmatrix} =$$

$$\begin{pmatrix} \frac{1}{\sqrt{2}}(\cos\varphi + i\sin\varphi\cos\theta) & \frac{-1}{\sqrt{2}}(\sin\varphi - i\cos\varphi\cos\theta) & \frac{-1}{\sqrt{2}}i\sin\theta \\ \sin\varphi\sin\theta & \cos\varphi\sin\theta & \cos\theta \\ \frac{1}{\sqrt{2}}(\cos\varphi - i\sin\varphi\cos\theta) & \frac{-1}{\sqrt{2}}(\sin\varphi + i\cos\varphi\cos\theta) & \frac{1}{\sqrt{2}}i\sin\theta \end{pmatrix} \begin{pmatrix} T_x \\ T_y \\ T_z \end{pmatrix}, \tag{3}$$

where the angles φ and θ define the direction of the magnetic field in the coordinate frame attached to the molecule.

The radiative deactivation rate constants k_+, k_0, k_- of the Zeeman sublevels (and the absorption coefficients ε_α proportional to them) are expressed in terms of the zero-field radiative deactivation constants k_x, k_y, k_z as follows:

$$k_\alpha = \sum_i |C_{\alpha i}|^2 k_i, \tag{4}$$

where the subscripts α and i assume the values $+$, 0, $-$ and x, y, z, respectively. The coefficients $C_{\alpha i}$ are determined by the 3×3 matrix in (3). It is clear from (3) and (4) that the constants $k_\alpha(\varphi, \theta)$ depend on the orientation of the molecule relative to the external magnetic field H.[2] However, we always have $k_+ = k_-$. Expression (4) can be used to calculate the probabilities k_x, k_y, k_z of radiative transitions for zero-field spin levels from experimental data on the Zeeman effect.

We now turn to line intensities and consider two essentially different situations.

2. Boltzmann equilibrium in the spin system. The population ratio of the spin sublevels (for each of the three laser-excited types of center) is now

$$n_+/n_0 = n_0/n_- = \exp(-g\beta H/kT) = A. \tag{5}$$

Since, in addition, the number of absorption events per Zeeman sublevel $\varepsilon_\alpha I$ (I is the excitation intensity) is equal to (under stationary excitation conditions) the number of radiative and nonradiative deactivations of all three sublevels to the state S_0, we can readily show that the intensities of the

lines in the quintet (Fig. 1b) are given by

$$I_1 = Ck_+{}^2 A^2, \quad I_2 = Ck_+ k_0 A(A+1), \quad I_3 = C[k_+{}^2(A^2+1) + k_0{}^2 A],$$

$$I_4 = Ck_+ k_0(A+1), \qquad I_5 = Ck_+{}^2; \tag{6}$$

$$C = \frac{IB}{A^2 k_+' + A k_0' + k_-'}, \quad B = \frac{\varepsilon_+}{k_+} = \frac{\varepsilon_0}{k_0} = \frac{\varepsilon_-}{k_-}.$$

The constants k'_+, k'_0, k'_- are the total rates of deactivation of the corresponding Zeeman sublevels to the state S_0, and represent both radiative and nonradiative processes. (These constants can, naturally, be regarded as the same for all three types of excited center.) The quantities k_α and C in (6) are functions of the angles φ and θ. This must be taken into account when one analyzes the intensity distribution in a Zeeman multiplet in the case of randomly oriented molecules (by taking the corresponding average). However, it is clear from (6) that the intensity ratio for two pairs of lines does not contain the above angular dependence:

$$I_2/I_4 = A, \qquad I_1/I_5 = A^2. \tag{7}$$

It will be shown below that (7) remains in force even in the absence of the Boltzmann distribution in the spin system. Hence, the criterion for identifying the presence or absence of equilibrium takes the form of the other two ratios, namely, I_3/I_4 and I_3/I_5, where the corresponding geometric factors must be taken into account (see below).

3. Absence of Boltzmann equilibrium. This situation is of particular interest in connection with the fact that, when there are appreciable deviations from equilibrium in the molecular spin system, we have the possibility of using spectroscopic data to determine the spin-lattice relaxation con-

stants (even under stationary excitation and recording of the spectra). To obtain the intensities of Zeeman components for this case, we must consider the set of three kinetic equations for the populations n_+, n_0, n_- of the Zeeman sublevels for each of the three types of center. In the approximation of linear reaction[10] of the ensemble of molecules in solution to a deviation from equilibrium, the set of kinetic equations (for stationary conditions) can be written in the form[3]

$$
\begin{pmatrix}
k_+{}'+x+y & -Ax & -A^2y \\
-x & k_0{}'+x(A+1) & -Ax \\
-y & -x & k_-{}'+Ax+A^2y
\end{pmatrix}
\begin{pmatrix}
n_+ \\
n_0 \\
n_-
\end{pmatrix}
= \left(f \right),
\tag{8}
$$

where the matrix on the right is given by

$$
\left(f \right) = \begin{pmatrix} \varepsilon_+ I \\ 0 \\ 0 \end{pmatrix}; \quad \begin{pmatrix} 0 \\ \varepsilon_0 I \\ 0 \end{pmatrix}; \quad \begin{pmatrix} 0 \\ 0 \\ \varepsilon_- I \end{pmatrix}
\tag{9}
$$

for each of the three types of excited center, respectively. The quantities $x = k_{+0}$ and $y = k_{+-}$ are the rates of thermal spin-lattice relaxation between Zeeman sublevels.

From (8), written in the appropriate form for each of the three types of excited center, we obtain the following expressions for the line intensities in the Zeeman quintet:

$$
I_1 = (IB/\Delta) A^2 k_+{}^2 (x^2+by), \quad I_2 = (IB/\Delta) A k_+ k_0 x (a+c+2Ay),
$$

$$
I_3 = (IB/\Delta) [k_+{}^2 (ab+bc-2Ax^2) + k_0{}^2 (ac-A^2y^2)],
$$

$$
I_4 = (IB/\Delta) k_+ k_0 x (a+c+2Ay), \quad I_5 = ('IB/\Delta) k_+{}^2 (x^2+by),
\tag{10}
$$

where Δ is the determinant of the 3×3 matrix in (8) and

$$
a = k_+{}'+x+y, \quad b = k_0{}'+x(A+1), \quad c = k_-{}'+Ax+A^2y.
\tag{11}
$$

It is clear from (10) that $I_1, I_2, I_4, I_5 \to 0$ when there is no spin-lattice relaxation (i.e., $x, y \to 0$), and the quintet is replaced by a single central line. In the other limiting transition $x, y \to \infty$ (Boltzmann equilibrium), the intensities given by (10) become identical with (6). (In this case, we must, of course, express Δ in terms of x and y.) As already noted, it is immediately clear from (10) that the relations given by (7) remain valid in the absence of equilibrium.

The expressions given by (7) and (10) can be used to analyze experimental data and, in particular, to determine the spin-lattice relaxation constants from spectroscopic data.

EXPERIMENTAL METHOD

In the experiment discussed below, the measurements were performed in the region of the purely electronic $T_1 \leftarrow S_0$ transition under excitation of phosphorescence in the same region by a narrow laser line. (Direct $T_1 \leftarrow S_0$ excitation is essential in this case because inhomogeneous broadening of the phosphorescence spectra is not removed by the usual $S_1 \leftarrow S_0$ excitation.[5]) The main difficulty in these experiments was that we had to record weak signals (in the region of the spin-forbidden $T_1 \leftarrow S_0$ transition, the absorption coefficient is lower by a factor of 10^5–10^6 than in the region of allowed transitions, so that the phosphorescence is excited with relatively low efficiency). In addition, scattered laser radiation must be completely excluded.
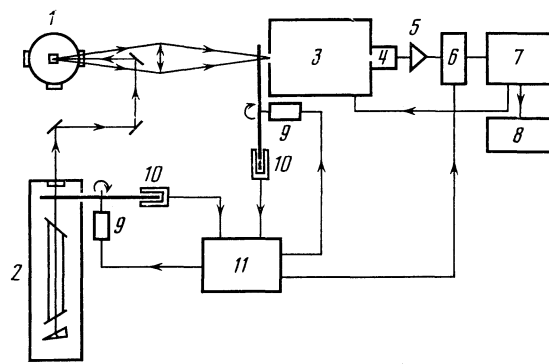

FIG. 2. Block diagram of the apparatus: 1—helium cryostat with superconducting solenoid; 2—Ar^+ laser (ILA-120) with a dispersive resonator; 3—DFS-24 monochromator; 4—photomultiplier; 5—biased amplifier; 6—electronic shutter; 7—automated system for the acquisition and analysis of data and the control of the experiment by the D-3-28 minicomputer; 8—graphplotter; 9—mechanical modulators (phosphoroscope); 10—synchronizing pulse generators; 11—phosphoroscope control unit.

A block diagram of the apparatus is shown in Fig. 2. The system incorporates a helium cryostat 1 with a superconducting solenoid, an Ar^+ laser 2 with a dispersive resonator, the DFS-24 spectrometer 3 with an automatic system 4–8 for recording and analyzing the spectra, and the two-shutter phosphoroscope 9–11.

The solution under investigation ($\sim 1{*}$ml) was in a quartz cell placed at the center of a vertical solenoid and was immersed in liquid helium. The cell was covered by an aluminum foil with an aperture through which radiation could enter and leave. Phosphorescence was excited through a side aperture in the solenoid, using laser radiation with wavelengths 4880 and 5145 Å ($\Delta v \sim 0.1$ cm^{-1}, power ~ 1.5 W). The phosphorescence leaving through the same aperture was focused on the spectrometer slit.

A special phosphoroscope was used to perform measurements at the excitation frequency and to ensure complete suppression of scattered laser radiation. It incorporated two mechanical modulators 9 rotated by a dc motor, and a synchronization system for the rotation of the motors 11. One of the modulators was placed in front of the spectrometer slit and the other in the interior of the laser resonator. The second modulator ensured that laser generation stopped within the time intervals in which phosphorescence was recorded (the length of the on-off cycle was varied in the range 0.1–0.001 s). The control unit 11 produced strict synchronization of the rotational phase of the motors and produced control pulses for the electronic shutter 6. The latter (used in addition to the mechanical shutter 9) cut off the recording channel whilst the specimen was being excited. This double protection was found to be necessary for the reliable recording of resonance fluorescence without the admixture of laser radiation scattered by parts of the apparatus.

The spectra were recorded by the photon counting method, using multiple scanning and digital data storage. The scanning of the spectrum and all the data storage and processing operations were performed by the D-3-28 computer. Multiple scattering was used as an efficient way of suppressing drift noise, which is important when the data acquisition times are long (slow misalignment of optical sys-

tem, laser power drift in time, and so on). By using long enough spectrum recording times, we were able, therefore, to obtain good-quality spectra for low signal intensities, and the spectra were suitable for detailed qualitative examination. The total signal acquisiton time per point was up to 2 min when the weaker spectra were recorded. The scanning step was 1/32 Å in all experiments. The spectral resolution was about 0.2 Å.

When experimental data are analyzed with the aid of (6) and (10), it is important to remember that the intensity distribution in the Zeeman quintet is sensitive to the direction of propagation and the polarization of the excited and recorded radiation relative to the field $\mathbf{H}$. In fact, the quantities k_α in (6) and (10) depend on the mutual orientation of the transition dipole moment μ_α and the direction of the polarization unit vector $\mathbf{e}$ of the incident radiation:

$$k_\alpha \sim |\mu_\alpha \mathbf{e}|^2 = k_{\alpha x'} e_{x'}^2 + k_{\alpha y'} e_{y'}^2 + k_{\alpha z'} e_{z'}^2, \tag{12}$$

where x', y', z' are defined relative to the laboratory coordinate frame. It follows that (especially when light-scattering specimens are employed) the "effective" values of k_α in (6) and (10) must be determined by averaging in (12) over the directions of the exciting and recorded radiation. This procedure is carried out independently of the averaging over orientations of the molecules. For example, when excitation (recording) is performed along the x' axis, it is readily shown that

$$\overline{e_{x'}^2} = {}^1\!/_3 - {}^1\!/_2 \cos \Omega (1 - {}^1\!/_3 \cos^2 \Omega),$$

$$\overline{e_{y'}^2} = \overline{e_{z'}^2} = {}^1\!/_3 (1 - \cos^3 \Omega / 4), \tag{13}$$

where Ω is the aperture angle.

In our experiments, we used highly-scattering specimens in "integrating sphere" type containers and an aperture angle $\Omega = \pi/2$. (We note that excitation and recording were performed along the x' axis; the field $\mathbf{H}$ was parallel to the z' axis.)

EXPERIMENTAL DATA AND DISCUSSION

General appearance of spectra. We have chosen coronene and 5-bromacenaphthene molecules (with very different triplet lifetimes) for our investigation. The $T_1 \leftarrow S_0$ absorption bands of these molecules lie in the frequency region corresponding to the strongest lines of the argon laser. The solvents were ethanol and butyl bromide.

Figure 3 shows the phosphorescence spectra of these molecules under two types of excitation. In both compounds, the transition from ordinary excitation to selective $T_1 \leftarrow S_0$ laser excitation leads to the appearance in the spectrum of a large number of narrow vibronic zero-phonon lines instead of broad bands $(\Delta \nu \sim 100 - 200 \text{ cm}^{-1})$. This confirms inhomogeneous broadening of the spectra and demonstrates that it is suppressed under selective excitation. The Zeeman experiments were performed with the narrowest and strongest purely electronic resonance lines of coronene (5145 Å) and 5-bromoacenaphthene (4880 Å).

The phosphorescence lines were found to split when the magnetic field was applied. As expected, the spectrum contained quintets due to the simultaneous excitation of three types of center in the inhomogeneous system (and to the partial superposition of the corresponding triplets) in which the separation between neighboring components was a linear function of the field H and amounted to about 0.94 cm^{-1}/ kOe (see Figs. 4 and 5 and their discussion below). The principal object of analysis in this case was the intensity distribution in the observed quintets. This requires the highest possible precision in measurements of the integrated line intensity.

In low fields ($H \lesssim 20$ kOe), measurements of the integrated intensity required the separation of the line profiles. In our case, the situation was simplified by the fact that the number of lines per multiplet was known, all the lines had the same shape, and the separation between them was the same. The profiles were separated by using different approximating functions (provided in tabulated form, and symmetric and asymmetric Gaussian curves), using the least-squares method with provision for a convergence check and an estimate of precision. The parameters of the approximating functions were first determined for the resonance phosphorescence line in zero field. The best results (convergence and minimum mismatch) were obtained when the profiles were approximated by an asymmetric Gaussian.

A precise value of the temperature was necessary for the analysis of experimental data. Special experiments showed that the presence of very small amounts of impurity (even less than 0.1%) capable of absorbing laser radiation in the region of the allowed $S_n \leftarrow S_0$ transitions produced a small amount of heating.[4] The temperature was therefore determined by the "internal thermometer" in the form of the two intensity ratios I_2/I_4 and I_1/I_5 (which, for given H, are func-
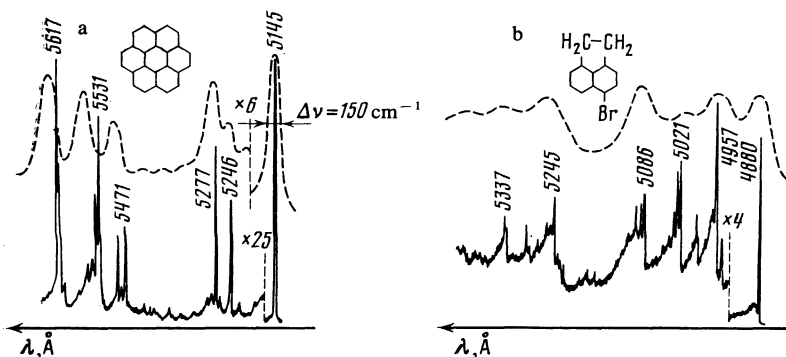

FIG. 3. Phosphorescence spectra of coronene (a) and 5-bromoacenaphthene (b) in butyl bromide under ordinary $S_1 \leftarrow S_0$ (dashed curves) and selective $T_1 \leftarrow S_0$ laser excitation (solid curves); $T = 4.2$ K.
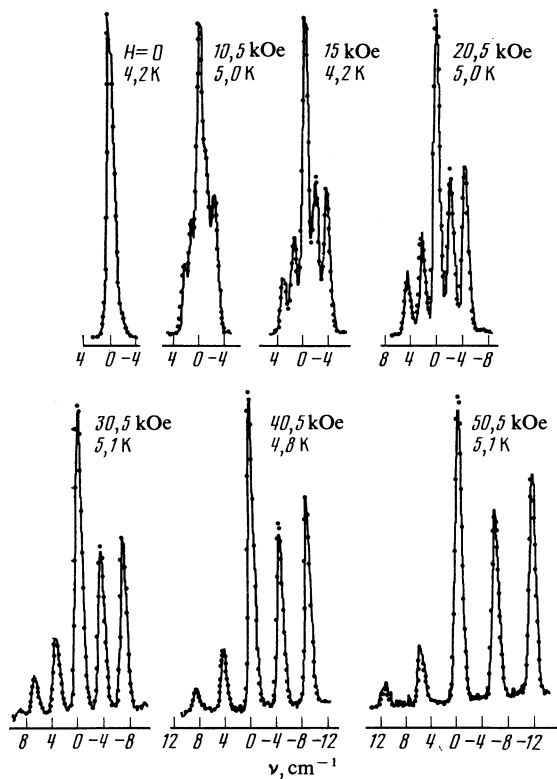
FIG. 4. Zeeman effect recorded using the 0–0 phosphorescence line of coronene in butyl bromide under $T_1 \leftarrow S_0$ laser excitation ($\lambda_{laser} = 5145$ Å). Solid curves—experimental, points—calculated from (6) for Boltzmann equilibrium. Field and temperature values are shown against the curves.
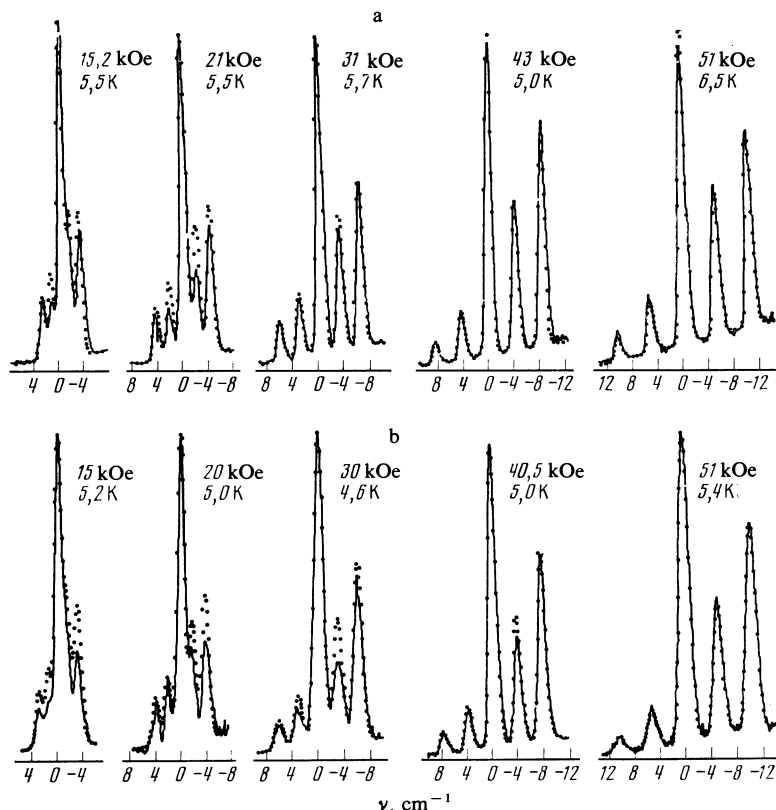
tions of temperature only).

Finally, we note one further point which is important in the analysis of the data. The degree of anisotropy of the quantities k'_+, k'_0, k'_-, which appear in the parameters a, b, c, and Δ in (10), depends on the ratio of the radiative and nonradiative deactivation constants, i.e., the phosphorescence quantum yield Φ. When $\Phi = 1$, we have $k'_\alpha = k_\alpha$, and the anisotropy is at a maximum, whereas for $\Phi \rightarrow 0$ the constant k'_α becomes isotropic. Numerical calculations have shown that this anisotropy is already small for $\Phi \sim 0.5$ and can be neglected when x and y are determined (within the range of uncertainty of our measurements). Hence, k'_α was assumed isotropic in our analysis of the experimental data (in which case, $k'_+ = k'_- = k'_0$).

The analysis of experimental data was aimed at determining the relative rates of radiative deactivation of zero-field spin sublevels k_i and, whenever the spin system was not in Boltzmann equilibrium, the rates of spin-lattice relaxation x and y.

Coronene. The Zeeman multiplets observed in the region of the purely electronic transition in the phosphorescence spectrum of coronene are shown in Fig. 4. Analysis of the intensity distribution in these multiplets shows that, throughout the field range (0–50 kOe) that we have investigated, the Boltzmann equilibrium prevails in the spin system. By varying the constants k_x, k_y, k_z within wide limits, we showed that the best agreement between the intensities calculated from (6) and the experimental data is achieved for the following two sets of constants: $k_x : k_y : k_z$

FIG. 5. Zeeman effect recorded using the 0–0 phosphorescence line of 5-bromacenaphthene under $T_1 \leftarrow S_0$ laser excitation ($\lambda_{laser} = 4880$ Å): a—in butyl bromide; b—in ethanol. Solid curves—experimental, points—calculated from (6) for Boltzmann equilibrium. Field and temperature values are shown against curves.

TABLE I. Relative integrated intensities of the laser quintet (in % of the integrated intensity I_3 of the resonance line) in the spectrum of 5-bromacenaphthene in ethanol for different values of the magnetic field.

H, kOe	T, K		I_1	I_2	I_4	I_5
10	4,5	experiment	11,7	11,3	15,5	21,2
		calculation	20,6	24,3	32,7	37,6
15	5,2	experiment	12,2	13,2	19,3	26,5
		calculation	18,6	22,9	33,9	40,4
20	5,0	experiment	10,1	16,0	27,6	30,1
		calculation	15,2	20,8	35,8	45,1
30	4,6	experiment	7,8	10,6	25,9	45,1
		calculation	9,5	16,4	39,4	56,0
40,5	5,0	experiment	6,6	11,8	35,1	60,4
		calculation	6,9	13,9	41,2	61,5
51	5,4	experiment	5,2	11,8	42,9	66,9
		calculation	5,2	11,8	42,9	66,9

Note: The experimental uncertainty in the intensities of well-resolved lines is about 2% of the integrated intensity I_3. For poorly resolved weak lines the uncertainty is up to 10% in individual cases. Calculations were performed on the basis of (6) for Boltzmann equilibrium.

$ = 1 : 0.4 : 0.1$ and $k_x : k_y : k_z = 1 : 0.3 : 0.3$. Both sets (established to within better than ± 0.1) ensure agreement between experiment and calculations to within experimental uncertainty for all fields.[5]

Coronene (whose triplet state has a relatively long lifetime $\tau_{phosph} \sim 1$ s) is thus an example of an object in which the time necessary to establish equilibrium in the spin system is small in comparison with the electronic-excitation deactivation time.

5-bromacenaphthene (BA). Figure 5a shows the Zeeman multiplets in the phosphorescence spectrum of BA in butyl bromide. As in coronene, these multiplets consist of five lines but, in the case of BA (for which the lifetime of the triplet is relatively short: $\tau_{phosph} \sim 0.01$ s), the intensity distribution in the multiplets and its dependence on H turn out to be more complicated. Even qualitative analysis shows that the Boltzmann distribution is not present in the spin system of BA (this is seen, in particular, in the relatively low intensities of the nonresonance lines, I_2 and I_4). As the field increases, the spin system approaches equilibrium. In the case of BA (and in contrast to coronene), we are able to determine the rates x and y (as well as k_i). However, simultaneous determination of the constants k_x, k_y, k_z and the spin-lattice relaxation rates x and y from experimental data was not possible because, for any given intensity distribution in the multiplet, one can find a number of sets of k_i and values of x and y they are uniquely related to them for which (10) gives the required result. Thus, if there is no Boltzmann equilibrium in the spin system of the molecule, the equilibrium must be set up in some way (for example, by increasing the field or temperature), and the ratios k_i must be determined under these conditions. Comparison of numerical calculations with experimental data shows that equilibrium obtains for fields $H \gtrsim 40$ kOe and a departure from it begins to be appreciable for $H \sim 30$ kOe (see Fig. 5a). Using (4) and (6) with the data for $H = 51$ kOe, we have found (to within ± 0.1) that $k_x : k_y : k_z = 1 : 0.2 : 0$.

Since we have found a departure from equilibrium in the spin system of BA in butyl bromide, it was interesting to perform a similar study for a different host. When ethanol was used as the solvent, we found somewhat greater deviations from the Boltzmann equilibrium, which increased with decreasing field (Fig. 5b). These deviations were appreciable even for $H \sim 40$ kOe. However, analysis shows that, when $H \approx 50$ kOe, the system may be regarded as practically in Boltzmann equilibrium. The result obtained from the data for $H = 41$ kOe was[6] $k_x : k_y : k_z = 1 : 0 : 0$. The measured and calculated (for the Boltzmann case with the above con-

TABLE II. Rates of spin-lattice relaxation in solutions of 5-bromoacenaphthene in different magnetic fields.

In butyl bromide $(1/k'_\alpha \approx \tau_{phosph} = 0,021$ s$)$				In ethanol $(1/k'_\alpha \approx \tau_{phosph} = 0,025$ s$)$			
H, kOe	T, K	x/k'_α	y/k'_α	H, kOe	T, K	x/k'_α	y/k'_α
10,5	5,0	0,5–3	2,5–5	10	4,5	0,3–2	1–3
15,2	5,5	1–3	30–50	15	5,2	0,5–4	2–5
21	5,5	1–3	40–70	20	5,0	3–11	0,1–10
31	5,7	9–11	$\gtrsim 10^2$	30	4,6	1,5–3	20–50
43	5,0	$\gtrsim 10^2$	$\gtrsim 10^2$	40,5	5,0	9–11	$\gtrsim 10^2$
51	6,5	$\gtrsim 10^2$	$\gtrsim 10^2$	51	5,4	$\gtrsim 10^2$	$\gtrsim 10^2$

Note. The precision of the values obtained for xEk'_α and y/k'_α in the range $H = 10$–30 kOe was determined by the precision with which the weak and highly overlapping line intensities I_4 and I_5 were determined. For H in the range 40–50 kOe, the precision with which the ratios x/k'_α and y/k'_α were determined was governed by the degree of deviation of the spin system from thermal equilibrium.

stants k_i) intensities of the components of the quintet in the spectrum of BA in ethanol are shown in Table I for different values of H. These data clearly illustrate the difference between the observed intensity distribution and the distribution expected in thermal equilibrium. The measured integrated intensities of the components of the quintet were then used to calculate the rates of spin-lattice relaxation for BA in ethanol and in butyl bromide. The results are listed in Table II.

It is clear from Table II that the values of x and y have a considerable spread. This is due to the fact that small errors in the measured intensities lead to much greater errors in the calculated values of x and y. (To obtain more accurate values, one would have to increase the precision of the measured intensities.) However, the data of Table II enable us to draw the following conclusions: (1) the rates of spin-lattice relaxation increase rapidly with increasing field (we note that similar behavior of these rates was established by other methods for certain mixed crystals[7,12]), the probable reason for this being that, as the separation between the Zeeman levels increases, there is an increase in the density of phonon states participating in the relaxation processes; (2) the rates of spin-lattice relaxation are different for different solvents, a reasonable conclusion because these processes must be strongly dependent on the phonon spectrum of the host and the nature of the electron-phonon interaction; (3) the relaxation constant y is always greater than x (for given H), so that the line intensities I_1 and I_5 reach equilibrium values more rapidly as the field increases. In addition to a possible difference between selection rules for the transitions, we also have the possibility that the principal factor is the difference between the sublevel separations. In fact, the constant y is responsible for transitions with $\Delta E = 2g\beta H$, and the constant x for transitions with $\Delta E = 2g\beta H$. If this assumption is valid, we should have $y(H) = x(2H)$. For example, y for $H = 10$ kOe should be equal to x for $H = 20$ kOe, and so on. This rule is approximately obeyed, but additional (and more accurate) experimental data will be necessary before reliable validation of this result can be performed.

CONCLUSION

The above data demonstrate new possibilities for Zeeman experiments with complex molecules. The method that we have proposed extends the range of objects accessible to detailed magnetooptical studies.

One of the important features of the method is the selective excitation directly in the region of the spin-forbidden $T_1 \leftarrow S_0$ transition. This direct excitation (and not the usually employed population of the triplet level as a result of intercombinational $S_1 \rightarrow T_1$ conversion after $S_1 \leftarrow S_0$ absorption) assures the absence from the corresponding kinetic equations of additional and unknown constants of intercombina-

tional conversion to Zeeman sublevels, which substantially simplifies the situation and the analysis of experimental data.

Our discussion and experimental examples demonstrate the fact that Zeeman experiments can be used to determine the constants of radiative intercombinational transitions, the spin-lattice relaxation rate, and its dependence on the medium, field, temperature, and so on. They also reveal new ways of obtaining information about the density of states of low-frequency phonons in the host.

---

1)The first term in (1) represents the energy of interaction between spin and external magnetic field, whereas the second gives the magnetic dipole interaction between two electrons, which determines the zero-field splitting of the level T_1.

2)This anisotropy is absent only for highly symmetric molecules for which $k_x = k_y = k_z$.

3)In this approximation, the number of relaxation transitions from a given sublevel to other sublevels (or vice versa) is proportional to the deviation of the population from the equilibrium value. For example, for the upper sublevel, the terms $-k_{+0}(n_+ - n_0 A)$ and $-k_{+-}(n_+ - n - A^2)$ are introduced into the equation for n_+.

4)Absorption by these molecules in the region of the spin-forbidden $T_1 \leftarrow S_0$ transition is negligible and cannot produce heating even at relatively high laser intensities.

5)The two sets of constants k_i, giving practically the same intensity distributions in the Zeeman quintet, arise when more than one component k_i, is different from zero. This experimental uncertainty is connected with disorder in the system.

6)Small differences between the k_i ratios for the same molecule in different solvents may be due to the effect of the heavy external halogen atom that modifies the spin-orbit interaction.

[1]S. McGlynn, T. Azumi, and M. Kinoshita, Molecular Spectroscopy of the Triplet State, Prentice Hall, 1969 [Russ. transl., Mir Moscow, 1972, Chapter 10].

[2]R. I. Personov, E. I. Al'shitz, and L. A. Bykovskaya, Pis'ma Zh. Eksp. Teor. Fiz. 15, 609 (1972) [JETP Lett. 15, 431 (1972)]; Opt. Commun. 6, (1972)].

[3]R. I. Personov, E. I. Al'shitz, L. A. Bykovskaya, and B. M. Kharlamov, Zh. Eksp. Teor. Fiz. 65, 1825 (1973) [Sov. Phys. JETP 38, 912 (1974)].

[4]R. I. Personov, "Site selection spectroscopy of complex molecules in solutions and its applications," in: Spectroscopy and Excitation Dynamics of Condensed Molecular Systems, North-Holland, Amsterdam, 1983, Chap. 10; Spectrochimica Acta B 38, 1533 (1983).

[5]E. I. Al'shitz, R. I. Personov, and B. M. Kharlamov, Chem. Phys. Lett. 40, 116 (1976); Opt. Spektrosk. 41, 803 (1976) [Opt. Spectrosc. (USSR) 41, 474 (1976)].

[6]E. I. Al'shitz, R. I. Personov, and B. M. Kharlamov, Pis'ma Zh. Eksp. Teor. Fiz. 26, 751 (1977) [JETP Lett. 26, 586 (1977)].

[7]V. M. Kharlamov, E. I. Al'shitz, R. I. Personov, V. I. Nishankovsky, and V. G. Nazin, Opt. Commun. 24, 199 (1978).

[8]B. M. Kharlamov, E. I. Al'shitz, and R. I. Personov, Opt. Commun. 44, 149 (1983).

[9]A. Carrington and A. D. McLachlan, Introduction to Magnetic Resonance with Applications to Chemistry and Chemical Physics, Harper and Row, 1967 [Russ. transl., Mir Moscow, 1970].

[10]D. N. Zubarev, Neravnovesnaya statisticheskaya termodinamika (Nonequilibrium Statistical Thermodynamics), Nauka, Moscow, 1971.

[11]M. S. De Groot, I. A. M. Hesselman, J. Schmidt, and J. H. Van der Waals, Mol. Phys. 15, 17 (1968).

[12]H. Sixl and M. Schwoerer, Chem. Phys. Lett. 6, 21 (1970).

Translated by S. Chomet

434   Sov. Phys. JETP 60 (3), September 1984

Kharlamov et al.   434